

# Gold on WSe<sub>2</sub> Single Crystal Film as a Substrate for Surface Enhanced Raman Scattering (SERS) Sensing

Bablu Mukherjee,<sup>1,2,†</sup> Wei Sun Leong,<sup>1,†</sup> Yida Li,<sup>1</sup> Hao Gong,<sup>3</sup> Ergun Simsek,<sup>2</sup> and John T. L. Thong,<sup>1,\*</sup>

<sup>1</sup>Department of Electrical and Computer Engineering, National University of Singapore, Singapore 117583.

<sup>2</sup>Electrical and Computer Engineering, School of Engineering and Applied Science, The George Washington University (GWU), Washington, DC 20052, USA.

<sup>3</sup>Department of Materials Science & Engineering, National University of Singapore, Singapore 117575.

*\*Corresponding author's e-mail: elettl@nus.edu.sg*

*†These authors contributed equally to this work.*

**ABSTRACT** We report the synthesis of high-quality single-crystal WSe<sub>2</sub> films on highly-insulating substrate. We demonstrate for the first time that the presence of gold nanoparticles in the basal plane of a WSe<sub>2</sub> film can enhance its Raman scattering intensity. The experimentally observed enhancement ratio in the Raman signal correlates well with the simulated electric field intensity using a three-dimensional electromagnetic software. This work provides guidelines for the use of two-dimensional WSe<sub>2</sub> films as a SERS substrate.

In the recent years, transitional metal dichalcogenide (TMD) materials have attracted tremendous attention due to their potential applications in valleytronics, flexible and low power electronics, optoelectronics and sensing devices<sup>1, 2, 3, 4, 5, 6</sup>. One of the TMD materials, tungsten diselenide (WSe<sub>2</sub>) has a structure of Se-W-Se covalently bonded in a hexagonal quasi-2D network configuration that is stacked by weak Van der Waals forces. It is a group VI TMD that exhibits a trigonal prismatic structure with an indirect band gap of 1.21 eV in the bulk form and which increases to 1.25 eV (direct) at monolayer thickness<sup>7</sup>. Besides having excellent electrical properties, WSe<sub>2</sub> shows great promise for optical sensing applications<sup>2, 3, 4, 8</sup>. Due to its exceptional optical properties, WSe<sub>2</sub> yields strong Raman signal compared to other TMD materials. Nevertheless, no work has reported that explores the potential of enhancing its Raman signal to render it a suitable surface-enhanced Raman spectroscopy (SERS) substrate. In view of SERS being a topic of growing research interest, substrate materials with strong Raman signal are being sought for sensing applications in analytical, biological and surface sciences.

In this work, we first synthesize large triangular/hexagonal WSe<sub>2</sub> single crystal films on c-face sapphire substrates *via* chemical vapor deposition (CVD) techniques. We demonstrate that the Raman signal of WSe<sub>2</sub> films can be enhanced easily by Au decoration making it a competitive SERS substrate for sensing device applications. An electromagnetic wave simulation was performed to quantitatively explain the experimentally observed enhancement in Raman scattering of our WSe<sub>2</sub> film arising from the Au decoration.

## Results and Discussion

We have been able to synthesize single crystal WSe<sub>2</sub> film continuous over a length of more than 170  $\mu\text{m}$ . Figure 1a illustrates the experimental setup that was used to grow the WSe<sub>2</sub> films on c-face sapphire substrate via a CVD approach (see Methods for details). Figure 1b shows a photograph of the test tube containing 0.3 grams of WSe<sub>2</sub> powder at its closed end while the sapphire substrate was placed about 4 cm away from the powder source. It is worth noting that the growth of WSe<sub>2</sub> films on c-face sapphire substrate is highly dependent on the substrate position and temperature. Apart from this, we also attempted

to grow WSe<sub>2</sub> films on both a- and r-face sapphire substrates, but there was no sign of growth on both types of the sapphire substrates. Figure 1c and the inset of Figure 1d show the optical images of our synthesized WSe<sub>2</sub> films, which appear reasonably uniform and exhibit either triangular or hexagonal shapes with a lateral dimensions of 100 to 200  $\mu\text{m}$ . In order to check the uniformity of the synthesized WSe<sub>2</sub> films, we performed a large area Raman scan using a WITec alpha 300R system with a 532 nm (2.33 eV) laser excitation source and a step size of 160 nm. The laser power at the sample was kept below 0.1 mW which did not give rise to noticeable sample heating. As can be seen from the inset of Figure 1d, the intensity map of the E<sub>12g</sub> band is uniform throughout the large triangular WSe<sub>2</sub> film with a lateral size of more than 170  $\mu\text{m}$ . In short, we have synthesized large triangular/hexagonal WSe<sub>2</sub> films on c-face sapphire substrates that are of uniform thickness.

In order to examine the number of layers of our CVD-grown WSe<sub>2</sub> films, we further characterized them through Raman analysis and atomic force microscopy. It has been reported that monolayer WSe<sub>2</sub> nanosheets on sapphire substrate show A<sub>1g</sub> mode vibration at 264  $\text{cm}^{-1}$  and two dominant peaks are observed around 250  $\text{cm}^{-1}$  in various samples from monolayer to bulk on SiO<sub>2</sub> (300 nm)/Si substrate<sup>5,9</sup>, while bulk WSe<sub>2</sub> exhibits two distinct Raman characteristic signals at 248 and 250.8  $\text{cm}^{-1}$  theoretically as well as experimentally<sup>10,11</sup>. Our as-synthesized WSe<sub>2</sub> film has two characteristic Raman peaks located at  $\sim 252 \text{ cm}^{-1}$  and  $\sim 260 \text{ cm}^{-1}$ , which can be assigned to the in-plane vibrational E<sub>12g</sub> mode and the out-of-plane vibrational A<sub>1g</sub> mode, respectively (Figure 1d). In addition, another prominent Raman band was detected at  $\sim 309 \text{ cm}^{-1}$  for our as-synthesized WSe<sub>2</sub> film, which is an indication of interlayer interaction for layered 2D material<sup>6</sup>. Furthermore, the thickness of our WSe<sub>2</sub> film is measured to be 1.6 nm (Figure S1), and hence we believe that our CVD-grown WSe<sub>2</sub> film is a bilayer.

We also observed crystallinity of our CVD-grown WSe<sub>2</sub> films in a transmission electron microscope (TEM). The TEM image in Figure 2a shows the periodic atom arrangement of the WSe<sub>2</sub> film, indicating that the WSe<sub>2</sub> film is highly crystalline. Figure 2b shows the selected area electron diffraction (SAED) pattern taken on the WSe<sub>2</sub> film with an aperture size of  $\sim 200 \text{ nm}$ . The high-resolution TEM image and its corresponding SAED pattern indicate hexagonal lattice structure with a spacing of 0.38 and 0.34 nm

that can be assigned to the (100) and (110) planes, respectively. Apart from that, the chemical composition of the synthesized film is determined to be tungsten (W) and selenium (Se) with an atomic ratio of 1:2 by using an energy-dispersive X-ray spectroscopy (EDX) detector that is attached to the TEM (Figure 2c). The carbon and copper peaks in EDX spectrum can be attributed to the thin carbon film and copper mesh of TEM grid holder, respectively. These findings confirmed that the synthesized film is a single crystal WSe<sub>2</sub> film.

Thus far, we have confirmed that our CVD-grown WSe<sub>2</sub> film on c-face sapphire substrate is a bilayer and single crystal, and more importantly, it shows prominent Raman characteristic peaks. In order to transform the synthesized WSe<sub>2</sub> film into a promising SERS substrate, we decorated it with gold particles *via* 2 simple steps: Au film deposition and annealing. A thin layer of Au film (5 nm (Figure S2)) was first deposited on the CVD-grown WSe<sub>2</sub> film, followed by annealing in an inert environment at 550 °C for 3.5 h to form Au nanoparticles (NPs) on the WSe<sub>2</sub> films (see Methods for details). Figure S3a shows the AFM image (height profile) of a WSe<sub>2</sub> film on sapphire substrate and covered by Au NPs. Higher magnification AFM image (Figure S3b) shows a clearer view of Au NPs with average size of ~ 40 nm in diameter, height of ~ 5 nm and separation between two particles ~ 40-60 nm, which were formed on the WSe<sub>2</sub> film. Figure 3a shows a high resolution Raman intensity map of the E<sub>2g</sub><sup>1</sup> band of a typical WSe<sub>2</sub> film that was half-decorated with Au nanoparticles. It is obvious that the Raman intensity of the Au-decorated WSe<sub>2</sub> film is higher compared to that of bare WSe<sub>2</sub> film. Figure 3b shows the Raman spectrum of both Au-decorated and bare WSe<sub>2</sub> films and its inset shows their relative intensity difference in E<sub>2g</sub><sup>1</sup>/A<sub>1g</sub>. Basically, the Raman intensity of the WSe<sub>2</sub> film has been enhanced by 1.5 times by Au nanoparticles. The increase in the E<sub>2g</sub><sup>1</sup>/A<sub>1g</sub> peak intensity ratio suggests that localized surface enhanced scattering occurs due to Au NPs on the WSe<sub>2</sub> film. On the other hand, Figure 3c shows the optical image of a typical hexagonal WSe<sub>2</sub> film fully decorated with Au nanoparticles, while Figure 3d shows its Raman intensity map of the E<sub>2g</sub><sup>1</sup> band. It can be clearly seen that the Raman intensity is uniform throughout the Au-decorated WSe<sub>2</sub> film. In brief, Au-decoration enhances Raman signal of WSe<sub>2</sub> film making it a more promising candidate for SERS sensing.

To further illustrate the SERS capability of Au-decorated WSe<sub>2</sub> film, we performed a set of simulations to investigate how electric field distribution is changed by the presence of Au NPs using Wavenology EM, a general-purpose 3D electromagnetic wave simulation software<sup>12</sup>. First, we calculate the electric field intensity on bare WSe<sub>2</sub> film, which is placed on top of a sapphire substrate. Second, we place Au NPs on top of the WSe<sub>2</sub> film and follow the same procedure. Periodic boundary conditions are applied at the  $\pm X$  and  $\pm Y$  boundaries. Perfectly matched layers are applied at the  $\pm Z$  boundaries. For the optical constants of gold, experimental values are used<sup>13</sup> rather than the Drude model to eliminate any concern regarding the selection of appropriate values for plasmon and relaxation frequencies. The source illumination is a p-polarized plane wave under normal incidence. For the complex refractive index of WSe<sub>2</sub>, prior experimental results reported<sup>14</sup> are utilized. The parameters used for simulation roughly follow the experimental parameters, where Au cylindrical NPs are assumed to have a height of 6 nm and a radius of 20 nm. The inter-particle spacing along the x- and y-axes are assumed to be 80 and 100 nm, respectively, as shown in Figure 4a. WSe<sub>2</sub> layer is assumed to be 2 nm thick. Figures 4c and b plot the distribution of the magnitude of the electric field intensity on the WSe<sub>2</sub> surface (at  $-40 < X < 40$  nm,  $-50 < Y < 50$  nm) at a wavelength of 532 nm with and without an Au NP, respectively. The maximum field enhancement is observed at the bottom of the Au NP, where the enhancement ratio is around 2. The average field enhancement ratio is 1.5, which is related to the Raman scattering enhancement<sup>15</sup> as seen in Figure 3d.

In summary, large WSe<sub>2</sub> films were synthesized on highly-insulating sapphire substrate using a CVD technique. We carefully examine the synthesized films using Raman spectroscopy, TEM, EDX and AFM and confirmed that our CVD-grown WSe<sub>2</sub> films on c-face sapphire substrate are single crystal bilayer WSe<sub>2</sub> films with prominent Raman characteristic peaks. We demonstrate that Raman signature of the WSe<sub>2</sub> films can be enhanced easily by Au decoration. The enhancement of field distribution in the basal plane of WSe<sub>2</sub> by simple decoration of Au nanoparticles is supported by an electromagnetic wave simulation. To sum up, gold on WSe<sub>2</sub> single crystal film holds promise as a SERS substrate which could be suitable for sensing application.

## Methods

**Growth and Characterization of WSe<sub>2</sub> Films.** In our experiments, the synthetic route is described as follows. Pure WSe<sub>2</sub> powder (Sigma Aldrich, purity 99.8 %) was used as source materials. C-face sapphire substrates were placed inside the one-end open quartz-glass tube, where small amount (~ 0.3 grams) of WSe<sub>2</sub> source powder was loaded at the closed end of the tube as shown in the picture (Figure 1b). The tube was inserted in a horizontal quartz tube placed in a conventional tube furnace such that the substrate was set at lower temperature region of the source powders and the distance between them was about 4 cm. Then the quartz tube was evacuated to a base pressure  $\sim 10^{-3}$  mbar for 2 h by a vacuum pump and subsequently was filled with the mixture of argon (Ar) with 5% H<sub>2</sub> gas. The gas was allowed to flow for 1 hr after flushing the tube 2-3 times. After that, the furnace was heated under the mixture gas of Ar and 5% H<sub>2</sub> at a flow rate of 100 sccm (standard cubic centimeters per minute). When the temperature reached 950 °C (heating rate: 30 °C min<sup>-1</sup>), the pressure of Ar carrier gas was maintained at  $\sim 2$  mbar during synthesis for 15 mins. After the reaction was terminated, the substrates were taken out when the temperature of the furnace cooled down to room temperature.

The morphology, structure and chemical composition of the as-synthesized nanostructures were characterized using atomic force microscopy (AFM, Veeco D3000 NS49 system), transmission electron microscopy (TEM, JEOL, JEM-2010F, 200 kV), energy-dispersive X-ray spectroscopy (EDX) equipped in the TEM and Raman spectroscopy. All Raman analysis in this study were performed using a Raman system (WITec alpha 300R) with a 532 nm laser excitation source and laser spot size of  $\sim 320$  nm (x100 objective lens with numerical aperture 0.9). The laser power at the sample was kept below 0.1 mW which did not give rise to noticeable sample heating.<sup>16</sup> All Raman mappings were conducted with a step size of 160 nm. The spectral resolution was  $\leq 1.5$  cm<sup>-1</sup> (using a grating with 1,800 grooves mm<sup>-1</sup>) and each spectrum was an average of 10 acquisitions (0.1 s of accumulation time per acquisition).

**Formation of Gold Nanoparticles on the CVD-grown WSe<sub>2</sub> Films.** A metal shadow mask was used such that some of the CVD-grown WSe<sub>2</sub> films on c-face sapphire substrates were partially exposed. Subsequently, Au film was directly deposited on the sample via thermal evaporation at a rate of 0.05 nm/s

for 3-5s at a chamber base pressure of  $3 \times 10^{-6}$  mbar, and the thickness of Au film was measured to be ~5nm by AFM (Figure S2). The sample was then annealed at 550 °C for 3.5 h in an Ar gas environment to allow formation of Au NPs on the CVD-grown WSe<sub>2</sub> films<sup>17</sup>. As can be seen in Figure S3, the size of each Au NP is ~ 40 nm in diameter with a spacing of 40-60 nm between NPs.

## References

1. Lin J, Li H, Zhang H, Chen W. Plasmonic Enhancement of Photocurrent in MoS<sub>2</sub> Field-Effect-Transistor. *Appl Phys Lett* **102**, 203109 (2013).
2. Ross JS, *et al.* Electrically Tunable Excitonic Light-Emitting Diodes Based On Monolayer WSe<sub>2</sub> P-N Junctions. *Nat Nanotechnol* **9**, 268-272 (2014).
3. Das S, Appenzeller J. WSe<sub>2</sub> Field Effect Transistors with Enhanced Ambipolar Characteristics. *Appl Phys Lett* **103**, 103501 (2013).
4. Zhao W, *et al.* Evolution of Electronic Structure in Atomically Thin Sheets of WS<sub>2</sub> and WSe<sub>2</sub>. *ACS Nano* **7**, 791-797 (2012).
5. Kai X, Zhenxing W, Xiaolei D, Muhammad S, Chao J, Jun H. Atomic-Layer Triangular WSe<sub>2</sub> Sheets: Synthesis and Layer-Dependent Photoluminescence Property. *Nanotechnology* **24**, 465705 (2013).
6. Huang J-K, *et al.* Large-Area Synthesis of Highly Crystalline WSe<sub>2</sub> Monolayers and Device Applications. *ACS Nano* **8**, 923-930 (2013).
7. Sahin H, *et al.* Anomalous Raman Spectra and Thickness Dependent Electronic properties of WSe<sub>2</sub>. *Phys Rev B* **87**, 165409 (2013).
8. Jones AM, *et al.* Optical Generation of Excitonic Valley Coherence in Monolayer WSe<sub>2</sub>. *Nat Nanotechnol* **8**, 634-638 (2013).
9. Zeng H, *et al.* Optical signature of symmetry variations and spin-valley coupling in atomically thin tungsten dichalcogenides. *Sci Rep* **3**, (2013).
10. Tonndorf P, *et al.* Photoluminescence emission and Raman response of monolayer MoS<sub>2</sub>, MoSe<sub>2</sub>, and WSe<sub>2</sub>. *Opt Express* **21**, 4908-4916 (2013).
11. Ding Y, Wang Y, Ni J, Shi L, Shi S, Tang W. First principles study of structural, vibrational and electronic properties of graphene-like MX<sub>2</sub> (M=Mo, Nb, W, Ta; X=S, Se, Te) monolayers. *Physica B: Condensed Matter* **406**, 2254-2260 (2011).
12. Simsek E. On the Surface Plasmon Resonance Modes of Metal Nanoparticle Chains and Arrays. *Plasmonics* **4**, 223-230 (2009).
13. Raki AD, Djuricic AB, Elazar JM, Majewski ML. Optical properties of metallic films for vertical-cavity optoelectronic devices. *Appl Opt* **37**, 5271-5283 (1998).
14. Li S-L, Miyazaki H, Song H, Kuramochi H, Nakaharai S, Tsukagoshi K. Quantitative Raman Spectrum and Reliable Thickness Identification for Atomic Layers on Insulating Substrates. *ACS Nano* **6**, 7381-7388 (2012).
15. Schedin F, *et al.* Surface-Enhanced Raman Spectroscopy of Graphene. *ACS Nano* **4**, 5617-5626 (2010).
16. Leong WS, Nai CT, Thong JTL. What Does Annealing Do to Metal-Graphene Contacts? *Nano Lett* **14**, 3840-3847 (2014).
17. Bowker M, *et al.* Encapsulation of Au Nanoparticles on a Silicon Wafer During Thermal Oxidation. *J Phys Chem C* **117**, 21577-21582 (2013).

# FIGURES

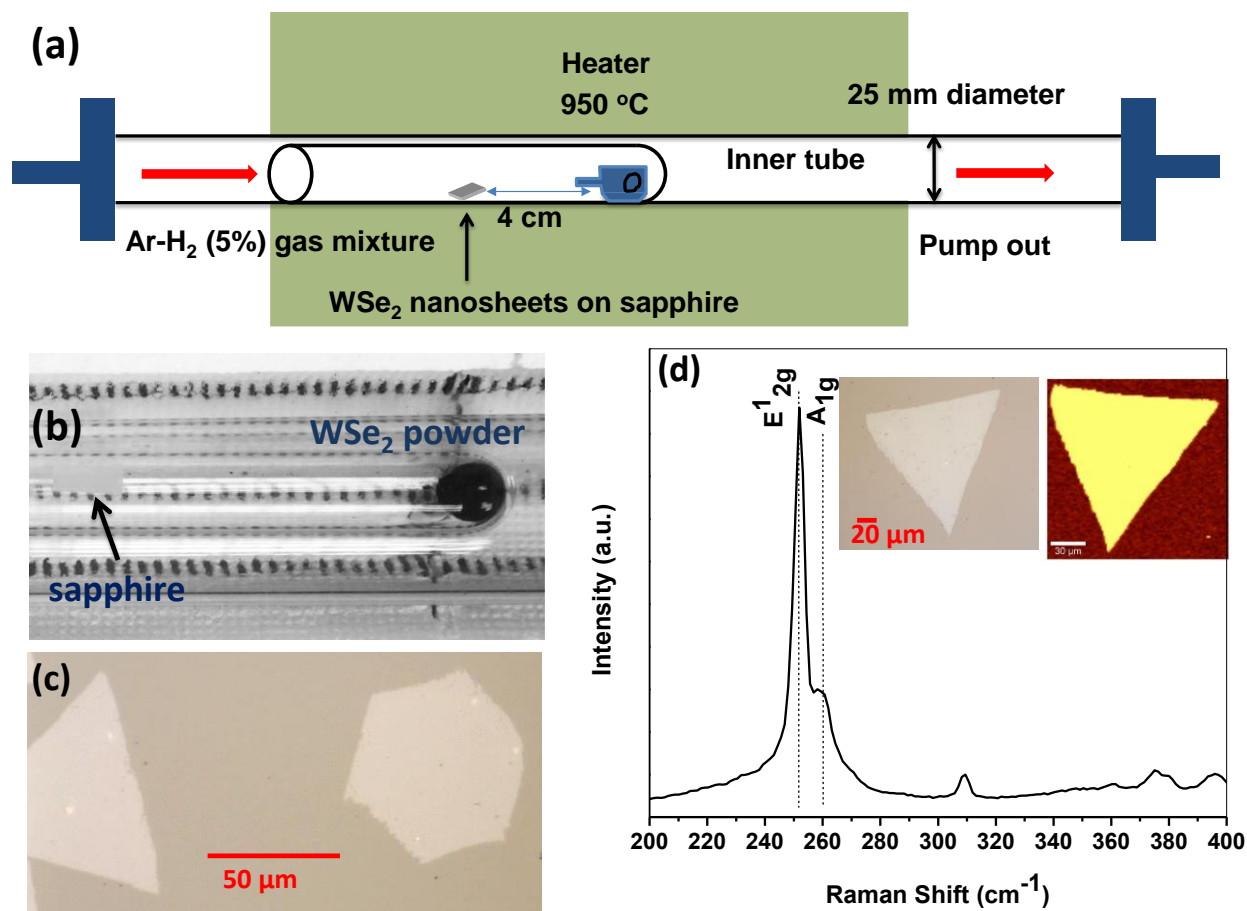


**Figure 1.** (a) Schematic representation of the experimental setup that we used to grow the WSe<sub>2</sub> films on c-face sapphire substrate. (b) Photo of the test tube containing 0.3 grams of WSe<sub>2</sub> powder at its closed end and the sapphire substrate was placed at about 4 cm away from the powder source. (c) Optical image of the typical as-synthesized WSe<sub>2</sub> films on a c-face sapphire substrate. (d) Raman spectrum of the typical WSe<sub>2</sub> film in its insets showing optical image of an individual WSe<sub>2</sub> triangular film (left) and the corresponding Raman intensity map of the E<sub>1</sub><sup>2g</sup> band (right).

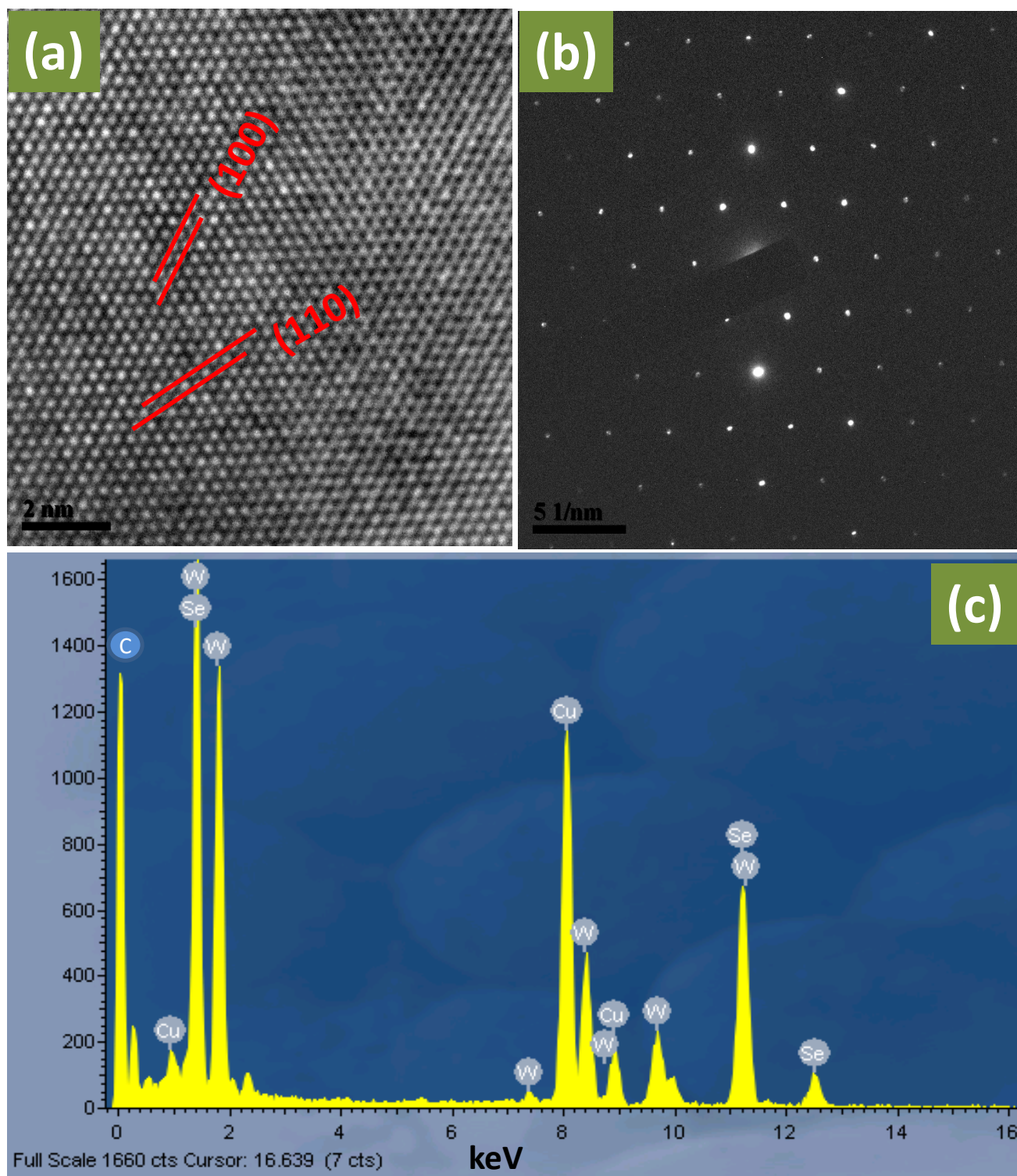


**Figure 2.** (a) High-resolution TEM image of a typical CVD-grown WSe<sub>2</sub> film. (b) The corresponding selected area electron diffraction (SAED) pattern. (c) Energy-dispersive X-ray (EDX) spectrum of the CVD-grown WSe<sub>2</sub> film.

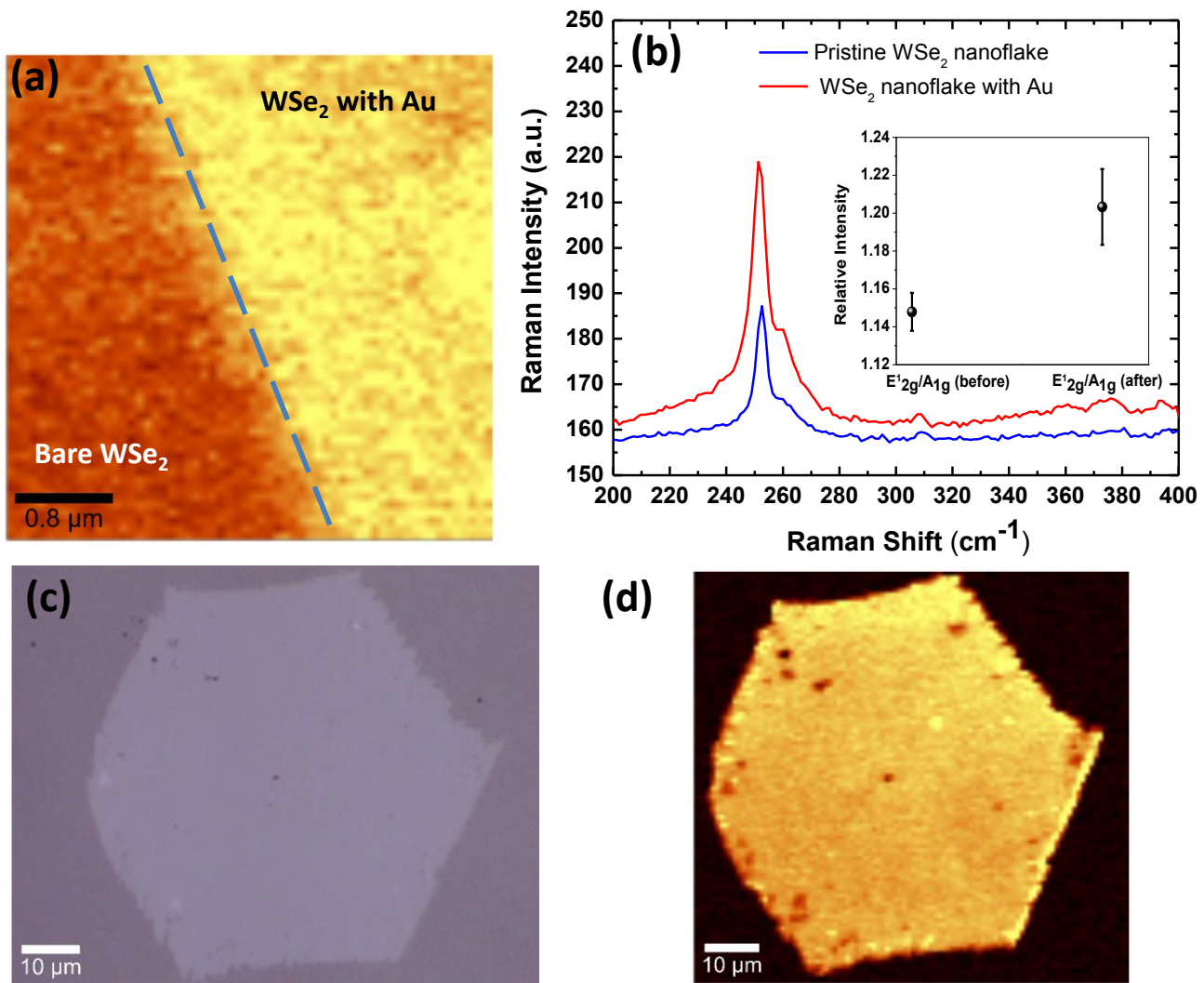


**Figure 3.** (a) High resolution Raman intensity map of the  $E'_{2g}$  band of a typical WSe<sub>2</sub> film that was half-decorated by Au nanoparticles. (b) Raman spectra of both Au-decorated and bare WSe<sub>2</sub> films and its inset shows their relative intensity difference in  $E'_{2g}/A_{1g}$ . (c) Optical image of a typical hexagonal WSe<sub>2</sub> film fully decorated by Au nanoparticles, and (d) its Raman intensity map of the  $E'_{2g}$  band.

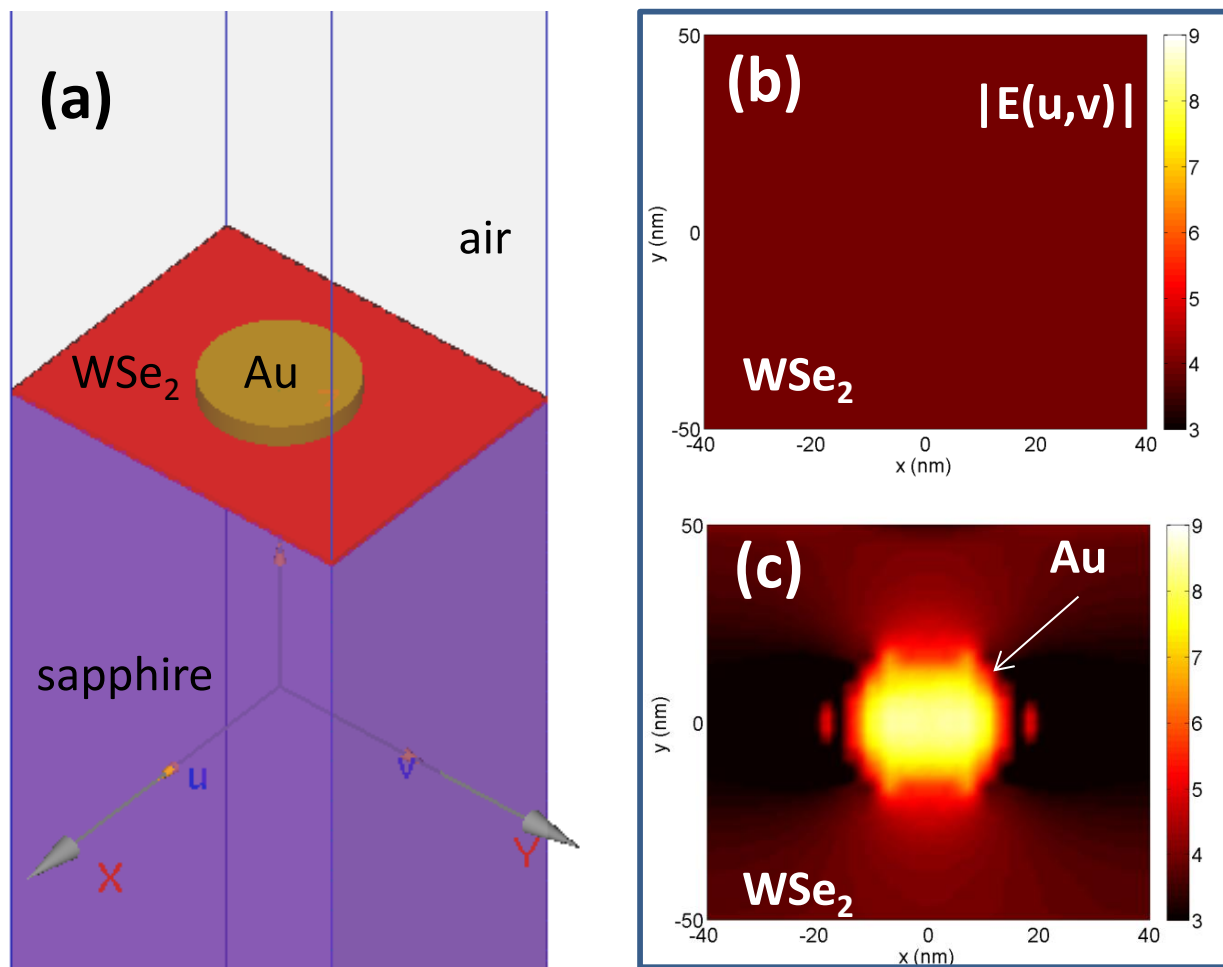


**Figure 4.** (a) Schematic diagram of the simulation box (with false color): 6 nm height Au cylindrical NP on a bilayer WSe<sub>2</sub> film (2 nm thick)/sapphire. The lateral periodicity is 80 nm and 100 nm along x and y axes of basal plane of the WSe<sub>2</sub>, respectively. We consider diameters of 40 nm for the cylindrical NP. (b, c) Simulated magnitude of the electric field distribution in the plane of interface between Au NP and WSe<sub>2</sub> film at a wavelength of 532 nm without and with Au NP configuration, respectively.